Air Force Institute of Technology
AFIT Scholar

Faculty Publications

7-2022

A Comparison of Correlation-Agnostic Techniques for Magnetic Navigation

Clark N. Taylor
Air Force Institute of Technology

Josh Hiatt
Air Force Institute of Technology

Follow this and additional works at: https://scholar.afit.edu/facpub

 Part of the Other Electrical and Computer Engineering Commons, and the Signal Processing Commons

Recommended Citation

Taylor, Clark N. and Hiatt, Josh, "A Comparison of Correlation-Agnostic Techniques for Magnetic Navigation" (2022). *Faculty Publications*. 976.
https://scholar.afit.edu/facpub/976

This Conference Proceeding is brought to you for free and open access by AFIT Scholar. It has been accepted for inclusion in Faculty Publications by an authorized administrator of AFIT Scholar. For more information, please contact richard.mansfield@afit.edu.

A Comparison of Correlation-Agnostic Techniques for Magnetic Navigation

Joshua Hiatt, Clark N. Taylor
Autonomy and Navigation Technology (ANT) Center
Air Force Institute of Technology
{jhiatt32, clark.n.taylor}@gmail.com

***Abstract*—Navigation using a Global Navigation Satellite System (GNSS) is common for autonomous vehicles (ground or air). Unfortunately, GNSS-based navigation solutions are often susceptible to jamming, interference, and a limited number of satellites. A proposed technique to aid in navigation when a GNSS-based system fails is magnetic navigation - navigation using the Earth's magnetic anomaly field. This solution comes with its own set of problems including the need for quality magnetic maps in every area in which magnetic navigation will be used. Many of the currently available magnetic maps are generated from a combination of dated magnetic surveys, resulting in maps riddled with spatially correlated errors, the correlation structure of which is largely unknown. The correlations are further confounded while navigating because they depend on how fast a vehicle moves through the map in addition to the original correlated error structure. Traditionally, this spatial correlation has been handled by introducing a First Order Gauss-Markov (FOGM) noise model into the estimation routine, with the FOGM parameters set somewhat arbitrarily. In this paper, we investigate the possibility of using correlation agnostic fusion techniques (i.e., Covariance Intersection and Probabilistically Conservative Fusion) for magnetic navigation. These techniques have the advantage of not requiring any parameter tuning; the same method and tuning parameters are used regardless of the spatial correlation. We demonstrate that utilizing probabilistically conservative fusion leads to navigation results that are better than many tuned approaches and reasonably close to the best possible tuning parameters of a FOGM.**

I. Introduction

Navigation techniques are constantly evolving. Throughout the centuries navigators have moved from simple piloting, dead reckoning, and celestial navigation to more sophisticated techniques such as electronic navigation using the Global Navigation Satellite System (GNSS). Regardless of the navigation technique, accurate pose (position, velocity, attitude) estimation must be performed for effective path-planning to take place. There is an ever-widening expanse of applications for a *robust* navigation framework in a wide variety of environments. GNSS-based navigation is incredibly accurate, but there are many scenarios for potential failure including but not limited to the following:

- Inside tunnels or in dense urban areas where satellite signals will be blocked.
- Frequency jamming and spoofing, which can cause the navigation solution to no longer receive accurate estimates. [1]

Due to the accuracy of GNSS, current alternative navigation systems do not attempt to replace GNSS, but to augment it in these potential failure situations. Current alternative navigation systems such as radio-based techniques, computer vision approaches, star-trackers, terrain height matching, and gravity gradiometry tend to only work in specific environments under certain conditions[2]. An alternative navigation system that can match the global *availability* of GNSS could improve and replace the plethora of current alternative navigation systems.

A promising navigation system that matches the availability of GNSS is magnetic navigation (Magnav) [2][3]. The availability of Magnav gives it an advantage over other alternative navigation solutions, but there are many challenges associated with Magnav that must be overcome including but not limited to the following:

- Availability of magnetic maps
- **Quality of magnetic maps including quality of metadata (co-variance, bias)**
- **Spatially correlated errors in the magnetic map leading to significant over-confidence in magnav-produced navigation estimates.**

This paper focuses on addressing the second and third point and is organized as follows. In Section II we give some background for Magnav and explain the problems that need to be overcome. In Section III, we explain our novel solution to modeling spatially correlated errors in an Extended Kalman Filter (EKF). Section IV mathematically defines the data fusion problem and reviews the Covariance Intersection and Probabilistically Conservative approaches to correlation agnostic data fusion. In Section V, we compare these techniques against each other. Section VI concludes the paper.

II. Background

Magnav uses the small variations in the Earth's magnetic anomaly field in order to navigate [4]. The anomaly field is available world-wide including over oceans, forests, and deserts - an attribute that vision-based and terrain height navigation systems lack. It is also available in all weather conditions unlike star-trackers. Recent successful flight tests have demonstrated scalar magnetic anomaly navigation to be a viable alternative navigation system and magnetic vector navigation could bring even more accuracy to Magnav [5][6].

A. Map Creation

Magnetic maps are generated through a process called Kriging, or Gaussian Process Regression (GPR) [7] [8]. Stated

simply, this process uses data from neighboring cells to estimate the data in a particular cell. This enables cells that do not have data to be filled in and improves the accuracy of cells that already have data. We used scikit-learn's GPR implementation for our testing [9]. While this process works remarkably well in approximating the true magnetic anomaly field, it (a) is not perfect and (b) introduces significant spatial correlation between its errors.

As an example, we generated a synthetic magnetic field and then processed that field, with sensor noise added, using GPR to create a representation (map) of that magnetic field. We tested various sampling patterns and different GPR parameters. We then took the difference between the resulting maps and the generated magnetic field (truth) to determine the map error. We then computed the power spectral density (PSD) of the error to analyze its spatial correlation structure. In Figure 1 we show the PSD of the errors for several different maps. If the noise was white (ideal for the filtering algorithms used in navigation), then the PSD would have the same value at all locations. Instead, as shown in Figure 1 there are significantly different values across the PSD, implying significant spatial correlation. Furthermore, the different sub-figures show that the correlation *structure* is significantly different depending on how the GPR is applied (the different kernel length sizes / subfigure (a) vs (b) and (c) vs (d)) *and* what data was sampled to create the map (which points were sampled / subfigure (a) vs (c) and (b) vs (d)). The presence of this correlation structure, if not properly handled by the filtering algorithm, leads to significant over-confidence in the derived pose estimates and larger errors in the final filter estimates.

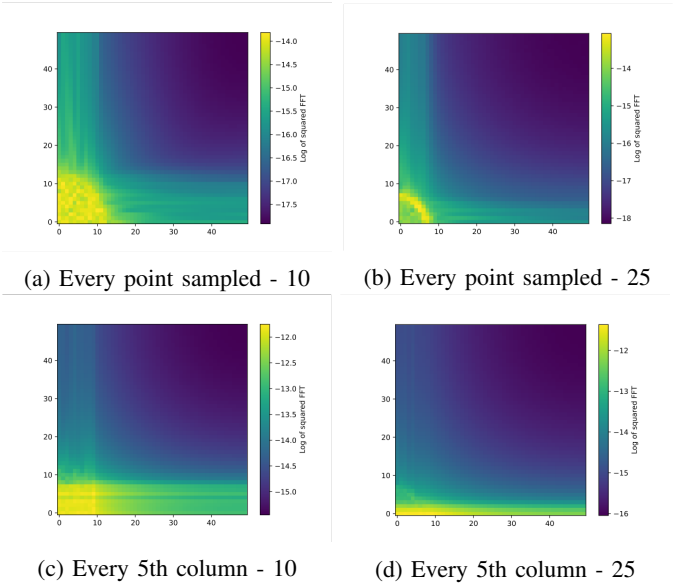

(a) Every point sampled - 10 (b) Every point sampled - 25

(c) Every 5th column - 10 (d) Every 5th column - 25

Fig. 1: PSDs of errors generated from various sampling patterns using a Kernel Length Size (KLS) of 10 and 25

Other map making techniques such as SLAM have also been used to create maps for Magnav [10] but these techniques are not explored in this paper because the dominant technique is the traditional GPR technique described above.

B. Filtering

A simple magnetic navigation filter is an Extended Kalman Filter (EKF) that uses a magnetic map and its derivative as part of the measurement processor to update the predicted pose of the vehicle. The standard EKF equations are used for prediction:

$$x^- = Fx + Bu \tag{1}$$
$$P^- = FPF^T + Q \tag{2}$$

where x^- is the predicted state, F is the system dynamics model, B is the control model, u is the control input, P^- is the predicted covariance, and Q is the covariance of the process noise. The update step is then performed:

$$y = z - h(x^-) \tag{3}$$
$$S = HPH^T + R \tag{4}$$
$$K = PH^T/S \tag{5}$$
$$x^+ = x^- + Ky \tag{6}$$
$$P^+ = (I - KH)P^- \tag{7}$$

where z is the measured magnetometer value, $h()$ is the magnetic value from the map given a predicted position[1], H is the derivative of the map at that point, and R is the covariance of the observation noise *plus* the covariance of noise in the map.

This filter would perform well if the errors in the maps were not correlated. However, as discussed, the errors are correlated in an unpredictable way. This will lead to significant over-confidence in pose estimates from a filter set up this way.

One way to overcome the sub-optimal performance of the filtering algorithms would be to accurately characterize the spatial correlation in the map and store it in meta-data. There are, however, two significant problems with this approach. First, many of the currently available magnetic maps are stitched together from previous surveys with varied quality [11]. Furthermore, these prior maps do not have any meta-data on the uncertainty of those maps. Second, even if new maps could be created, the exact interaction between sampling lines, the GPR process, and the spatial correlation of the magnetic field being sampled must all be considered to correctly characterize the spatial correlation at each point in the map. This is not a well-understood process and the metadata requirements could be extreme as every point could have a different spatial correlation structure from every other point.

If we eliminate high-accuracy prior estimation of spatial correlation in the map, this leaves two options for using magnetic map data in a navigation solution (1) Attempt to model the correlation in map errors using a coarse model or (2) use correlation agnostic fusion. In this paper we explore these two options. In the following sections, we first describe our method for modeling spatially correlated error using a first-order Gauss Markov Model, followed by a discussion of

[1]We are assuming the state x includes a position estimate that can be given to the magnetic map.

applying correlation agnostic fusion techniques to the magnav problem.

III. Modeling Approach

A. Problem Description

To derive a coarse model for spatial correlation, we choose to use the well-known first-order Gauss Markov model to model the correlation in the noise. This technique works by adding another state to the Kalman filter representing the correlated noise using the dynamics model:

$$\dot{\epsilon} = -\frac{1}{\tau}\epsilon + \nu \tag{8}$$

where τ is a time constant denoting how temporally correlated the noise source is ν is a white, Gaussian distributed noise source.

This technique, while straightforward, cannot be directly applied when performing estimation in the presence of spatial correlation. The process model in (8) correlated noise *temporally*, while the correlation in the map is *spatial*. Therefore, we must modify the process model for the correlated noise depending on the velocity of the vehicle as it moves through the spatially correlated map.

As an example, consider the 1-dimensional scenario shown in Figure 2. In subfigure (b) the error in the map is shown. Note that this error is not white and has significant spatial correlation. As the vehicle traverses the map, it has the velocity shown in subfigure (a). The resulting errors "observed" by the vehicle are shown in subfigure (c). Note how the errors in subfigure (c) seem spread out when the velocity is low and compressed when the velocity is high. More formally, higher velocity leads to lower temporal correlation while lower velocity leads to higher temporal correlation. Therefore, to properly perform estimation in the presence of spatially correlated noise, a pose estimation filter must account for the velocity dependent nature of the correlation.

B. Proposed Filter Modification

Consider the traditional prediction step of a Kalman Filter from equations 1 and 2 with three states (position, velocity, bias) assuming a First Order Gauss-Markov (FOGM) bias for the third term gives us:

$$F = \begin{bmatrix} 1 & \Delta t & 0 \\ 0 & 1 & 0 \\ 0 & 0 & e^{-\frac{\Delta t}{\tau}} \end{bmatrix} \tag{9}$$

$$Q_{[2,2]} = (1 - e^{\frac{-2\Delta t}{\tau}})\sigma_{ss}^2 \tag{10}$$

where Δt represents the change in time during the propagation step, σ_{ss} is the steady state, or total standard deviation of the bias, $Q_{[2,2]}$ represents the bottom right entry of a 3×3 matrix (we are using 0-indexing), and the other values of Q will be set appropriately for the filter.

To modify the Kalman filter to consider spatial correlation, we assume that the spatial correlation constant (Γ – the spatial equivalent of τ) is known. We then modify the traditional Kalman Filter equations to incorporate $d := distance$ to the

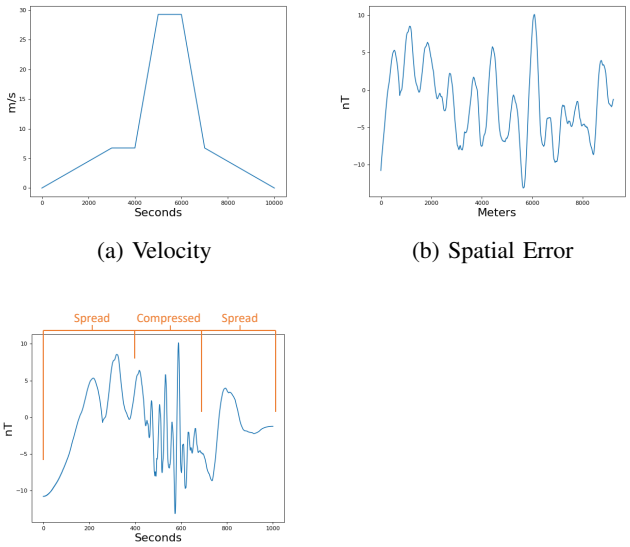

(a) Velocity

(b) Spatial Error

(c) Temporal Error

Fig. 2: The velocity dependence of correlated errors over time. The errors are spread out when velocity is low and compressed when velocity is high.

entry corresponding to the bias state in F and Q so that equations 9 and 10 change to:

$$F_{[2,2]} = e^{\frac{-d}{\Gamma}} \tag{11}$$

$$Q_{[2,2]} = (1 - e^{\frac{-2d}{\Gamma}})\sigma_{ss}^2 \tag{12}$$

Note, however, that d is not know, but must be estimated from the current velocity ($x[1]$) using:

$$d = x[1]\Delta t \tag{13}$$

While this modification is fairly straightforward, it has several important implications. First, because the process model is now dependent on the current state, this is now an Extended, rather than a linear Kalman filter. Second, it assumes that the correlation structure (σ_{ss}^2 and Γ) are known *and* can be approximated as a FOGM. Unfortunately, how to determine the "correct" Γ terms for a map is not immediately obvious. Also note that as we move beyond a simple 1d case, the Γ will most likely have a directional component to it, so both the numerator and denominator of the exponential terms will become dependent on the state.

Due to these difficulties with the FOGM model, we also wanted to investigate the possibility of using correlation agnostic fusion techniques to utilize measurements from the map. In this case, the accuracy or inaccuracy of any noise model for the map becomes far less important. How to utilize correlation-agnostic fusion for magnetic anomaly based navigation is the focus of the next section.

IV. Fusion Approach

The fusion problem in this paper is considering sequential measurements from a scalar magnetometer to determine the location of the magnetometer. Each update in a sequential

estimator consists of (1) predicting a measurement using the current estimated location and a magnetic map and (2) comparing this predicted measurement with a physical measurement from a magnetometer. The current location is then corrected using the difference between those two quantities (the predicted and physical measurements). Due to the use of a map for computing the predicted measurement, the error sources for the predicted measurement are not conditionally independent given the current location (the underlying assumption of sequential estimators). To overcome this lack of conditional independence, correlation agnostic fusion techniques can be used.

To use correlation agnostic fusion for magnetic anomaly navigation, we must combine two sources of information about the magnetic field magnitude (a scalar quantity measured in nanoTeslas); each providing a probability distribution function (PDF) representing its knowledge (labeled p_a and p_b). Assuming both distributions are Gaussian, the distributions can be completely represented by the mean (μ) and covariance matrix (P) associated with that distribution. Therefore, we have (μ_a, P_a) and (μ_b, P_b) representing the two input distributions to be fused. In the remainder of this section, we briefly review two correlation-agnostic methods for fusing together these distributions, followed by how this fused result is used by a sequential estimator.

A. Covariance Intersection Fusion Algorithm

Given two Gaussian input distributions, Covariance Intersection (CI) [12] returns for the covariance matrix the convex combination of the two information (inverse covariance) matrices of the two inputs [13]. Given the input means (μ_a, μ_b) and covariances(P_a, P_b), we can find the fused distribution based on CI using the following equations.

$$P_{fus}^{-1} = \omega_a P_a^{-1} + \omega_b P_b^{-1} \tag{14}$$

$$\mu_{fus} = P_{fus}(\omega_a P_a^{-1}\mu_a + \omega_b P_b^{-1}\mu_b) \tag{15}$$

$$\omega_a + \omega_b = 1 \tag{16}$$

where ω represents the weight for each input distribution. The selection of ω is usually based on an optimization the minimizes some metric (typically the determinate or trace) of the output covariance matrix. For example, if the determinate is used, we find ω as:

$$\omega := \underset{w}{\operatorname{argmin}} |P_{fus}| \tag{17}$$

B. Probabilistically Conservative Fusion Algorithm

While methods like CI consider only the input covariances to determine how to fuse two input distributions, Probabilistically Conservative Fusion (PC) [14] also uses the mean values to perform fusion. PC fusion is based on the assumption that p_a and p_b can be divided into independent (e.g., $p_{a\backslash c}$) and common distributions p_c:

$$p_a = p_{a\backslash c} p_c$$
$$p_b = p_{b\backslash c} p_c$$

but each distribution is still a sample distribution of the true value. When two input distributions are given to PC, the independent means for $p_{a\backslash c}$ and $p_{b\backslash c}$ should be close enough together that they can reasonably (probabilistically) be derived from the same quantity. "Close enough" is defined by a Mahalanobis distance $\Psi(P_c)$ compared with a chi-squared statistic as follows:

$$\Psi(P_c) = (\mu_{a\backslash c} - \mu_{b\backslash c})^\top (P_{a\backslash c} + P_{b\backslash c})^{-1} (\mu_{a\backslash c} - \mu_{b\backslash c}) \tag{18}$$

$$\Psi(P_c) \leq \chi^2_{n,.95} \tag{19}$$

where $\chi^2_{n,.95}$ denotes an chi-squared distribution with n degrees of freedom and .95 is the significance value used in this paper (though different values can be selected.) Note that n is the number of dimensions in the input distributions. PC then optimizes for the maximum amount of common information such that the two independent distributions satisfy the above constraint.

$$\begin{aligned} P_c^{-1} = & \underset{P_c^{-1}}{\operatorname{argmax}} |P_c^{-1}| \\ & s.t.\ \Psi(P_c) \leq \chi^2_{n,.95} \\ & P_c \leq P_a \\ & P_c \leq P_b \end{aligned} \tag{20}$$

where $P_c \leq P_a$ means that $P_a - P_c$ is a positive semi-definite matrix. PC has the advantage that even if the two input covariances are the same, if the means are different, some extra information can be derived from fusing the two inputs.

C. Fusion Methodology

In this paper, we investigate the use of Kalman-filter based estimators to estimate position and velocity using spatially correlated maps. For the prediction step of the Kalman filter, two approaches are used. If using a FOGM-based model, an extra state is added to the Kalman filter and the modifications described in Section III are used. When performing correlation-agnostic fusion, however, the state vector is not modified and the propagate step of the Kalman Filter is unaltered. The update step of the Kalman filter is modified though as shown in Algorithm 1. The modification performs correlation-agnostic fusion between the predicted and measured distributions, then generates a "synthetic" measurement and covariance. This synthetic measurement is generated such that the standard Kalman filter update step achieves the same measurement mean and covariance that would be obtained by running our chosen fusion method. Note that naïve Bayesian fusion is equivalent to an unmodified Kalman filter update.

The generic fusion process is described in Algorithm 1.

V. Simulation and Analysis

In order to compare different fusion techniques and the FOGM-based model, we created a simple 1-dimensional magnetic navigation simulation. This problem is based on [15] where a train is navigating on a track and the (1d) position and velocity of the train is estimated comparing scalar

Algorithm 1: Modified Kalman Filter Update for Magnetic Map Navigation

Result: $\boldsymbol{x}^+$, $\boldsymbol{P}^+$
Input: $\boldsymbol{x}^-, \boldsymbol{P}^-, z, R$
Generate predicted measurement distribution:
  $\mu \leftarrow h(\boldsymbol{x}^-)$
  $\boldsymbol{P}_p \leftarrow \boldsymbol{H}\boldsymbol{P}^-\boldsymbol{H}^\top$
Compute synthetic measurement:
  $\mu_f, P_f \leftarrow$ **fusion**(μ, P_p, z, R)
  $R_s \leftarrow (P_f^{-1} - P_p^{-1})^{-1}$
  $z_s \leftarrow R_s(P_f^{-1}\mu_f - P_p^{-1}\mu)$
Update state based on synthetic measurement (Standard Kalman filter update)
  $y \leftarrow z_s - h(\boldsymbol{x}^-)$
  $S \leftarrow \boldsymbol{H}\boldsymbol{P}\boldsymbol{H}^{\boldsymbol{T}} + R_s$
  $\boldsymbol{K} \leftarrow (\boldsymbol{P}\boldsymbol{H}^{\boldsymbol{T}})/S$
  $\boldsymbol{x}^+ \leftarrow \boldsymbol{x}^- + \boldsymbol{K}y$
  $\boldsymbol{P}^+ \leftarrow (\boldsymbol{I} - \boldsymbol{K}\boldsymbol{H})\boldsymbol{P}^-$

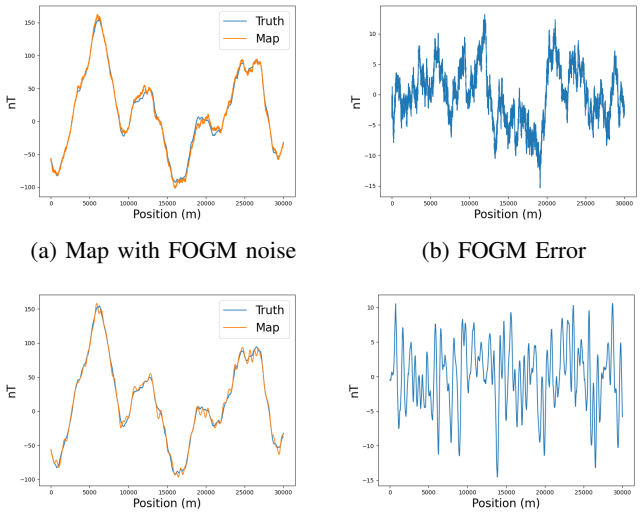

(a) Map with FOGM noise (b) FOGM Error

(c) Map with GPR noise (d) GPR error

Fig. 3: Example maps and errors used in 1-dimensional navigation simulation

magnetometer measurements against a magnetic map. Without biases, the system state consists of position and velocity, with an accelerometer being used as an input to modify the velocity. A Kalman-filter based estimator is tested using both the FOGM and correlation-agnostic fusion modifications described in Sections III and IV, respectively.

For the magnetic map, we generated synthetic maps in two ways: (1) With FOGM noise on the map - when we know the structure of the correlated map error perfectly - and (2) by sampling the truth map and creating a reconstructed map with GPR - when we can only attempt to model the structure of the correlated map error. While the overall variance of the errors is the same, the structure can be quite different. Example maps and errors from these two scenarios are shown in figure 3.

Maps were generated for 100 runs and each technique was used for navigation with the exact same inputs. Using these generated maps as well as noisy accelerometer measurements, we attempted to predict position, velocity, and covariance for 1000 seconds. In order to compare these techniques two metrics were used:

1) Root mean squared error (RMSE) of position – evaluates accuracy of technique. Lower is better.
2) Average Normalized Estimation Error Squared (ANEES) – evaluates accuracy of covariance outputs. If ANEES is less than 1, uncertainty is being overestimated. If it is greater than 1, uncertainty is being underestimated. While accuracy is the ideal outcome (ANEES $\approx$ 1), it is generally better to overestimate uncertainty (ANEES $<$ 1) than to underestimate it (ANEES $>$ 1).

These metrics were calculated for each technique as follows:

$$RMSE = \sqrt{\frac{1}{N}\sum_{i=0}^{N}(\boldsymbol{x}_{t_i}[0] - \boldsymbol{x}_{p_i}[0])^2} \tag{21}$$

$$\boldsymbol{e}_i = \boldsymbol{x}_{t_i} - \boldsymbol{x}_{p_i} \tag{22}$$

$$ANEES = \frac{1}{N}\sum_{i=0}^{N}\boldsymbol{e}_i^T\boldsymbol{P}_i^{-1}\boldsymbol{e}_i \tag{23}$$

where N is the number of time steps, $\boldsymbol{x}_{t_i}$ is the true state at time i, $\boldsymbol{x}_{p_i}$ is the predicted state at time i, $\boldsymbol{P}_i$ is the predicted covariance at time i, and $\boldsymbol{x}[0]$ is the first element in the state vector (position). The average of these values over 100 Monte Carlo simulations for each technique can be seen in Tables I and II. The rows of the table correspond with the following techniques:

- **Accelerometer Only (Baseline):** This technique performs no update steps in the Kalman filter, using only the process model and noisy accelerometer inputs to estimate location
- **FOGM EKF (Assumed Params):** This technique models a FOGM bias in the map. For FOGM map noise (columns) the assumed bias parameters are exact while for GPR map noise they are estimated. For the GPR maps, the Γ value was set equal to the kernel length used to generate the map.
- **FOGM EKF (Param Grid Search):** This technique is the same as the "FOGM EKF (Assumed Params)" except for the GPR columns, a grid search was performed to find the best combination of σ_{ss} (total standard deviation) and Γ (spatial correlation) to get optimal navigation accuracy. This technique is infeasible in the real world, but serves as a best-case metric against which to compare the correlation agnostic techniques. Both FOGM models use the technique described in Section III.

- **Bayesian (Naive):** This technique is Naive Bayes fusion. It is a traditional Kalman filter update with no bias in the state. It does not account for correlated errors in any way.
- **Covariance Intersection:** This technique is a fusion technique based on Covariance Intersection described in Section IV. It uses input covariances to determine how to fuse two distributions.
- **Probablisticly Conservative ($\alpha = 0.05$):** This technique is a fusion technique described in Section IV. It uses input covariances as well as input means to fuse two distributions. α corresponds to a significance value of 0.95, which is used to determine how fusion is performed

The columns of the table represent the following map errors:

- **FOGM:** First Order Gauss-Markov error with a total standard deviation of 5 nanoTesla and a τ (spatial correlation) of 1000 meters.
- **GPR-250:** Synthetic map generated by sampling the true map every 250 meters then recreating a map using GPR.
- **GPR-500:** Maps generated by sampling every 500 meters.
- **GPR-1000:** Maps generated by sampling every 1000 meters.
- **GPR-Random:** Maps generated by drawing one random sample within each 500m of the map.

In addition to the RMSE and ANEES error metrics, Figure 4 shows the average covariance bound for each technique. These bounds give more context to the values in Table I and II

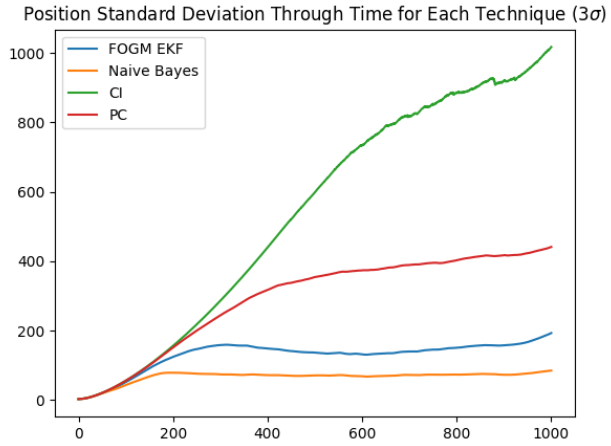

Fig. 4: Average covariance bounds for each technique

There are a few clear takeaways from the simulation:

- FOGM correlation model does exceptionally well when the structure of the error is FOGM and known perfectly but loses accuracy and underestimates uncertainty when applied to a GPR error structure.
- The weaknesses of the FOGM correlation model can be remedied by a grid search of potential models at the expense of computation time. This is infeasible for real-life scenarios[2]
- Naïve Bayes Fusion gives relatively good estimates regardless of the error structure but fails to predict the variance of the error accurately. This can be seen by how low the covariance bound is.
- Covariance Intersection relies heavily on accelerometer measurements instead of the map. The position estimates drift quite a bit before being corrected.
- CI has a high average RMSE yet very low ANEES because the covariance bound is so large.
- Probabilistically Conservative Fusion gives good estimates regardless of the correlated error structure. For cases where the spatial correlation is not known, it has the best results of the methods that are practically feasible. They are also not significantly worse than our "best case" scenario (FOGM EKF – Param Grid Search option). Its ANEES values are also reasonable, showing it accurately estimates the covariance bound for all error structures.

VI. Conclusion

A major problem in magnetic navigation is dealing with unknown correlations in magnetic maps. This paper has outlined multiple approaches for dealing with these unknown correlations. One of these approaches is a novel technique that incorporates velocity into the bias state of an Extended Kalman Filter. This technique is very accurate if the error structure is perfectly known, but struggles if the structure can only be approximated. Since the error structure of current maps is completely unknown, we investigated the possibility of using correlation agnostic fusion. Correlation agnostic techniques work regardless of the error structure, but tend to be less accurate than a perfectly tuned coarse model. Using a simulated train navigation scenario, we showed that PC fusion obtains good results regardless of the correlation structure, approaching results achieved by searching for the best possible FOGM model for a particular map and traversal of the map. In the future, we plan to test these techniques on real-world data including 2-dimensional maps and paths.

References

[1] C. Sebastian, "Getting lost near the kremlin? russia could be 'gps spoofing'." [Online]. Available: https://money.cnn.com/2016/12/02/technology/kremlin-gps-signals/

[2] A. Canciani, "Afit scholar theses and dissertations student graduate works absolute positioning using the earth' s magnetic anomaly field," 2016. [Online]. Available: https://scholar.afit.edu/etd/251

[3] C. Yang, J. Strader, Y. Gu, A. Canciani, and K. Brink, "Cooperative navigation using pairwise communication with ranging and magnetic anomaly measurements," 5 2020. [Online]. Available: http://arxiv.org/abs/2005.09541 http://dx.doi.org/10.2514/1.I010785

[4] A. Canciani and J. Raquet, "Airborne magnetic anomaly navigation," *IEEE Transactions on Aerospace and Electronic Systems*, vol. 53, 2017.

[5] A. Canciani and K. Brink, "Improved magnetic anomaly navigation accuracy through cooperative navigation," vol. 2017-May. The Institute of Navigation, 2017, pp. 239–262.

[6] A. Canciani and C. J. Brennan, "An analysis of the benefits and difficulties of aerial magnetic vector navigation," *IEEE Transactions on Aerospace and Electronic Systems*, vol. 56, pp. 4161–4176, 12 2020.

[2]The best FOGM is chosen by repeatedly trying different navigation filters and comparing against the truth. In a 2d map, different paths through the map would also need to be tried. This would be considerably more work than generating a new map!

TABLE I: RMSE for each technique with different error structures

	FOGM	**GPR-250**	**GPR-500**	**GPR-1000**	**GPR-Random**
Accelerometer Only (Baseline)	222.50	237.53	222.08	235.50	222.82
FOGM EKF (Assumed Params)	38.77	58.71	59.20	74.55	64.10
FOGM EKF (Param Grid Search)	38.64	38.25	48.41	67.10	53.23
Bayesian (Naive)	60.85	48.86	65.08	91.13	73.71
Covariance Intersection	105.09	84.54	108.12	134.76	116.68
Probablistic Conservative ($\alpha = 0.05$)	49.22	48.68	53.60	71.84	57.37

TABLE II: ANEES for each technique with different error structures

	FOGM	**GPR-250**	**GPR-500**	**GPR-1000**	**GPR-Random**
Accelerometer Only (Baseline)	0.979	0.91	0.97	0.87	0.91
FOGM EKF (Assumed Params)	0.78	3.23	1.38	1.42	2.23
FOGM EKF (Param Grid Search)	0.87	0.82	0.97	0.89	0.76
Bayesian (Naive)	4.70	4.23	5.63	9.23	8.40
Covariance Intersection	0.73	0.69	0.81	0.74	0.77
Probablisticly Conservative ($\alpha = 0.05$)	0.63	0.68	0.72	0.79	0.81

[7] C. E. Rasmussen and C. K. I. Williams, *Gaussian processes for machine learning*. MIT Press, 2006.

[8] R. Saltus, A. Chulliat, B. Meyer, and C. Amante, "Uncertainty estimation for magnetic maps," in *EGU General Assembly Conference Abstracts*, 2021, pp. EGU21–3541.

[9] scikit learn. Gaussian process regression (gpr). [Online]. Available: https://scikit-learn.org/stable/modules/generated/sklearn.gaussian_process.GaussianProcessRegressor.html

[10] T. N. Lee and A. J. Canciani, "Magslam: Aerial simultaneous localization and mapping using earth's magnetic anomaly field," *Navigation, Journal of the Institute of Navigation*, vol. 67, pp. 95–107, 3 2020.

[11] R. Saltus, B. Meyer, A. Chulliat, and C. Amante, "Uncertainty quantification for magnetic field maps and models," in *AGU Fall Meeting Abstracts*, vol. 2020, 2020, pp. NG002–0013.

[12] "General decentralized data fusion with covariance intersection (CI)," *Multisensor Data Fusion*, p. 269–294, 2001.

[13] S. J. Julier, "A non-divergent estimation algorithm in the presence of unknown correlations."

[14] A. Naveen and C. Taylor, "Decentralized data fusion with probabilistically conservative ellipsoidal intersection," in *2021 American Control Conference (ACC)*, 2021, pp. 1613–1618.

[15] B. Siebler, O. Heirich, S. Sand, and U. D. Hanebeck, "Joint train localization and track identification based on earth magnetic field distortions," 2020.